# Contribution of the partial ring current to the SYMH index during magnetic storms

H. Li,[1] C. Wang,[1] and J. R. Kan[1,2]

Received 27 May 2011; revised 31 August 2011; accepted 7 September 2011; published 29 November 2011.

[1] To identify which magnetospheric current system contributes the most to the SYMH index during magnetic storms, we performed a statistical analysis of 299 magnetic storms from 1996 to 2006 and investigated the distribution of the H depressions with magnetic local times (MLT), by using data from 25 geomagnetic stations distributed almost uniformly in magnetic longitudes over magnetic latitudes ranging from 9° to 45°. As expected, a significant dawn-dusk asymmetry of H depression during the storm main phase and early recovery phase reveals the importance of the partial ring current during magnetic storm processes. The location, evolution, and quantitative contribution of the partial ring current during magnetic storms with different intensities are all further obtained. The partial ring current locates in the dusk sector, peaking in 18:00~20:00 MLT. It forms in the early main phase, increases gradually until the SYMH index reaches its minimum, and then quickly decreases in the recovery phase. The contribution of the partial ring current weakens gradually as the storm intensity increases. For moderate ($-100 <$ SYMH $\leq -50$ nT) and intense ($-300 <$ SYMH $\leq -100$ nT) storms, the partial ring current is the predominant contributor during the main phase. However, the partial ring current is no longer the predominant contributor for the super storms with SYMH $\leq -300$ nT, which may suggest the saturation of the partial ring current under extreme solar wind conditions.

**Citation:** Li, H., C. Wang, and J. R. Kan (2011), Contribution of the partial ring current to the SYMH index during magnetic storms, *J. Geophys. Res.*, *116*, A11222, doi:10.1029/2011JA016886.

## 1. Introduction

[2] Geomagnetic storm is a global phenomenon involving the whole magnetosphere from the Earth's surface to distant magnetotail. Typically, a magnetic storm can last for 1 to 3 days, in which a global depression of the magnetic field is observed by the low-latitude and midlatitude geomagnetic stations. Geomagnetic storms have been studied for more than a century. Many investigations are dedicated to this phenomenon and greatly enrich our understanding. *Maltsev* [2004] has summarized all the large-scale magnetospheric currents which can contribute to the variations of horizontal component of geomagnetic field (H variations or H depressions, for short) observed on the ground. The major four of them are (1) the magnetopause current, (2) the symmetric ring current, (3) the cross-tail current, and (4) the partial ring current. The four closed current systems have different origin, topology, and effect as sketched by *Maltsev and Ostapenko* [2002a, Figure 4]. However, there is still much controversy on which magnetospheric current contributes the most to Dst variation in the study of magnetic storms.

[3] The magnetopause current usually causes an enhancement of geomagnetic fields. Thus the observed global geomagnetic depression is not associated with it.

[4] Different authors have made different estimations on the contribution of the symmetric ring current to the storm-time H depressions, ranging from 0 to 40%. With the statistical study of AMPTE observations about 80 storm events, *Greenspan and Hamilton* [2000] suggested that the symmetric ring current could hardly be considered as the principal cause of geomagnetic depression. Their results were indirectly supported by *De Michelis et al.* [1999]. However, the statistical study of particle observations on board the Polar satellite by *Turner et al.* [2001] gave somewhat different results. Their results implied that the symmetric ring current provided ~75% contribution to Dst under small disturbances (Dst $> -50$ nT), and ~40% for Dst $\sim -100$ nT.

[5] Even greater discrepancy exists concerning the contribution of the cross-tail current, with the estimations varying from 25% to 80%. *Turner et al.* [2000] evaluated the contribution of the cross-tail current to be ~25% for Dst $\sim -100$ nT. Somewhat larger contribution (~50%) was obtained in the work by *Alexeev et al.* [1992, 1996, 2001]. *Belova and Maltsev* [1994] and *Dremukhina and Feldstein* [1999] both found that the contributions of the cross-tail

[1]State Key Laboratory of Space Weather, Center for Space Science and Applied Research, Chinese Academy of Sciences, Beijing, China.
[2]Geophysical Institute, University of Alaska Fairbanks, Fairbanks, Alaska, USA.


0148-0227/11/2011JA016886

and ring current to Dst are nearly equal. However, 70 to 80% contribution of the cross-tail current to Dst were obtained by *Maltsev and Ostapenko* [2002a, 2002b] and *Maltsev* [2004].

[6] The discrepancy of the partial ring current contribution is also big, with the estimations varying from 15% to 80%. *Maltsev* [2004] obtained ~15% contribution of the partial ring current to Dst, allowing for the induced currents inside the Earth. However, *Liemohn et al.* [2001a, 2001b] found that most of the ring current (>90%) during the main phase and early recovery phase was partial rather than symmetric, closing through field-aligned currents into the ionosphere. *Le et al.* [2004] constructed the statistical magnetic field maps and derived three-dimensional current density by examining the 20 years of magnetospheric magnetic field data from ISEE, AMPTE/CCE, and Polar missions. They found that the partial ring current was three times of the symmetric ring current under moderate magnetic storms.

[7] According to the injection model, first proposed by *DeForest and McIlwain* [1971], the ring current is highly asymmetric in the main phase and early recovery phase of a magnetic storm and becomes symmetric in the later recovery phase. This phenomenon was interpreted traditionally in terms of the dusk-centered partial ring current [e.g., *Fukushima and Kamide*, 1973]. However, *Crooker and Siscoe* [1974] found that most of the disturbance field comes from the near-Earth part of the field-aligned portion of the current loop. *Crooker and Siscoe* [1981] further discussed a systematic twisting between the region 1 and region 2 currents as the cause of the asymmetric component to the low-latitude magnetic perturbation.

[8] *Weygand and McPherron* [2006] utilized 1-min resolution SYMH and ASYH indices [*Iyemori et al.*, 1992] to study the dependence of ring current asymmetry on storm phase. The ratio of -SYMH/ASYH was used to reflect the degree of ring current asymmetry. They found that the ratio is close to 1.0 in the main phase, implying that the symmetric and partial ring currents grow together. While in the recovery phase, the ratio increases continuously until it becomes meaningless, which implies that the main phase current system is converted to a symmetric ring as the ring current decays.

[9] The location of the partial ring current is still not completely understood. Traditional models of the partial ring current centered near dusk are successful in reproducing the observed low-latitude dawn-dusk asymmetry [e.g., *Cummings*, 1966; *Kamide and Fukushima*, 1971; *Crooker and Siscoe*, 1974]. The distribution of the partial ring current pressure is thought to peak in the dusk sector, based on ground-based measurements of H variations [e.g., *Shi et al.*, 2006].This was supported by the ring current modeling from global simulations [e.g., *Ebihara et al.*, 2002; *Jordanova et al.*, 2003]. Statistical analyses of magnetic depression maps of the inner magnetosphere from CRRES, ISEE, AMPTE/CCE, and Polar missions also showed that the partial ring current peaks in the dusk sector [*Lui*, 2003; *Le et al.*, 2004; *Jorgensen et al.*, 2004]. *Anderson et al.* [2005] obtained the similar results by analysis of the magnetometer data from the Iridium constellation of satellites.

[10] However, some new findings from IMAGE and TWINS missions challenge the traditional pictures. ENA images showed that the ring current ion fluxes in some particular energy ranges sometimes peak near the postmidnight sector during the main phase of magnetic storms [e.g., *Brandt et al.*, 2002; *Fok et al.*, 2003; *Ebihara and Fok*, 2004; *Perez et al.*, 2004; *Buzulukova et al.*, 2010]. This phenomenon is called postmidnight enhancement (PME). *Fok et al.* [2003] attributed this to a twisting of equipotential arising from shielding effects and an ionospheric conductivity gradient near the terminator.

[11] The explanation of the difference between location of the partial ring current peak and ENA peak, given by *Buzulukova et al.* [2010], is based on the dependence of the charge-exchange cross section with energy. *Buzulukova et al.* [2010] showed that PME is formed in a particular energy range depending on the strength of the storm. They also concluded that PME is often produced by ions with energies below ~16 keV for moderate storms and ~60 keV for strong storms, while most of the ring current pressure is produced by ions with energies above ~16 keV for moderate storms and ~60 keV for strong storms. Some studies have also quantified the effects of substorm current system on the magnetic perturbations at low latitudes and midlatitudes [e.g., *Clauer and McPherron*, 1974; *Friedrich et al.*, 1999; *Munsami*, 2000; *Clauer et al.*, 2003].

[12] In the study of magnetic storms, which magnetospheric current system contributes the most to the Dst index is still a highly debatable issue. In this work, we will quantitatively estimate the contribution of the partial ring current for different developing stages of magnetic storms, based on the observations of the dawn-dusk asymmetry of H variations. The data are from 25 geomagnetic stations distributed almost uniformly in magnetic longitudes over magnetic latitudes ranging from 9° to 45°. The remainder of this paper is organized as follows: The data set and methodology are briefly introduced in section 2. The observations of the dawn-dusk asymmetry and estimations of the partial ring current contribution to *Dst* are presented in section 3 and 4, respectively. The discussion and summary are given in section 5 and 6.

## 2. Data Set and Methodology

[13] Midlatitude magnetic variations have been often used as tools for the study of the ring current evolution during magnetic storms. Similar to the hourly Dst index [*Sugiura and Kamei*, 1991], the 1-min resolution SYMH index [*Iyemori et al.*, 1992] has being widely used as the measure of ring current's intensity to describe geomagnetic disturbances. The ASYH index [*Iyemori et al.*, 1992], the range between the maximum and the minimum deviation at each moment for the H component, is simultaneously introduced to represent the longitudinally asymmetric geomagnetic disturbances, which could be regarded as a measure of the partial ring current's strength. However, only six ground magnetometer stations unevenly distributed in longitude and latitude around the world are used for the derivation of the ASYH index. The error for the asymmetric geomagnetic disturbance must not be overlooked. Meanwhile, the ASYH index is not enough to reflect the location of asymmetry in detail.

[14] To obtain a more accurate correlation between the H variations and magnetic local times (MLTs), we choose

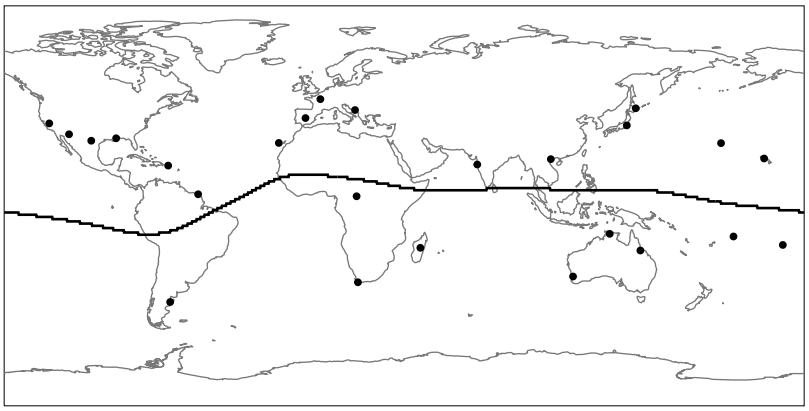

**Figure 1.** Distribution of the geomagnetic stations. The black line denotes the magnetic equator.

25 stations (from www.intermagnet.org) in low and middle magnetic latitudes, ranging from 9 to 45°, to cover magnetic longitudes as uniformly as possible. At lower and higher latitudes the contributions of the equatorial and auroral electrojets could distort the results. The distribution of the 25 stations is shown in Figure 1. The black dots represent the locations of the stations, and the solid curve represents the magnetic equator. Table 1 provides the names and locations in geographic and corrected geomagnetic coordinates of the above 25 stations.

[15] For a given station, we can calculate its magnetic local time at each moment. At the same time, the northward component of the geomagnetic field perturbation is obtained from the following formula:

$$\Delta H = \frac{H - H_q}{\cos\varphi} \tag{1}$$

where $\varphi$ is the magnetic latitude of the station, $H$ is the northward component of geomagnetic field, and $H_q$ is the same component of solar quiet variation, averaged over the 5 quietest days of that month. We can then obtain the mean H variation at each moment as follows:

$$\Delta H_m = \frac{1}{N}\sum_{n=1}^{N} \Delta H \tag{2}$$

where $n$ is the station number and $N$ is the total number of stations. Note that the derivation is close to the method described by *Clauer et al.* [2006] and *Love and Gannon* [2009, 2010] but is different from the standard calculation of the Kyoto SYMH and ASYH indices, which divide by the cosine of the average latitude of the stations rather than the individual station latitude.

**Table 1.** Geomagnetic Observatories

| Station Name | IAGA Code | Geographic Latitude | Geographic E Longitude | CGM Latitude | CGM Longitude |
|---|---|---|---|---|---|
| Trelew | TRW | −43.30 | 294.70 | −29.94 | 4.92 |
| San Juan | SJG | 18.10 | 293.80 | 27.46 | 10.73 |
| Kourou | KOU | 5.20 | 307.30 | 9.46 | 23.62 |
| Guimar-Tenerife | GUI | 28.30 | 343.60 | 17.17 | 60.51 |
| San Pablo-Toledo | SPT | 39.50 | 355.60 | 31.90 | 71.78 |
| Chambon la Foret | CLF | 48.00 | 2.30 | 43.33 | 79.10 |
| Hermanus | HER | −34.40 | 19.20 | −42.33 | 82.90 |
| Bangui | BNG | 4.30 | 18.60 | −8.71 | 90.39 |
| Tihany | THY | 43.10 | 17.90 | 37.28 | 91.46 |
| Antananarivo | TAN | −18.90 | 47.30 | −28.65 | 116.67 |
| Alibag | ABG | 18.60 | 72.90 | 12.08 | 145.46 |
| Phuthuy | PHU | 21.00 | 106.00 | 14.16 | 177.96 |
| Gnangara | GNA | −31.80 | 116.00 | −44.00 | 187.29 |
| Kakadu | KDU | −12.60 | 132.50 | −21.73 | 204.86 |
| Kakioka | KAK | 36.20 | 140.20 | 29.31 | 212.04 |
| Memambetsu | MMB | 43.90 | 144.20 | 37.12 | 215.74 |
| Charters Towers | CTA | −20.10 | 146.30 | −29.08 | 220.48 |
| Midway Island | MID | 28.20 | 182.60 | 24.77 | 250.23 |
| Apia | API | −13.80 | 188.20 | −15.60 | 262.65 |
| Honolulu | HON | 21.30 | 202.00 | 21.32 | 270.06 |
| Pamatai | PPT | −17.60 | 210.40 | −16.72 | 285.42 |
| Fresno | FRN | 37.10 | 240.30 | 42.98 | 303.97 |
| Tucson | TUC | 32.20 | 249.20 | 39.76 | 314.86 |
| Del Rio | DLR | 29.30 | 259.20 | 38.57 | 326.88 |
| Stennis Space Center | BSL | 30.40 | 270.40 | 41.20 | 340.95 |

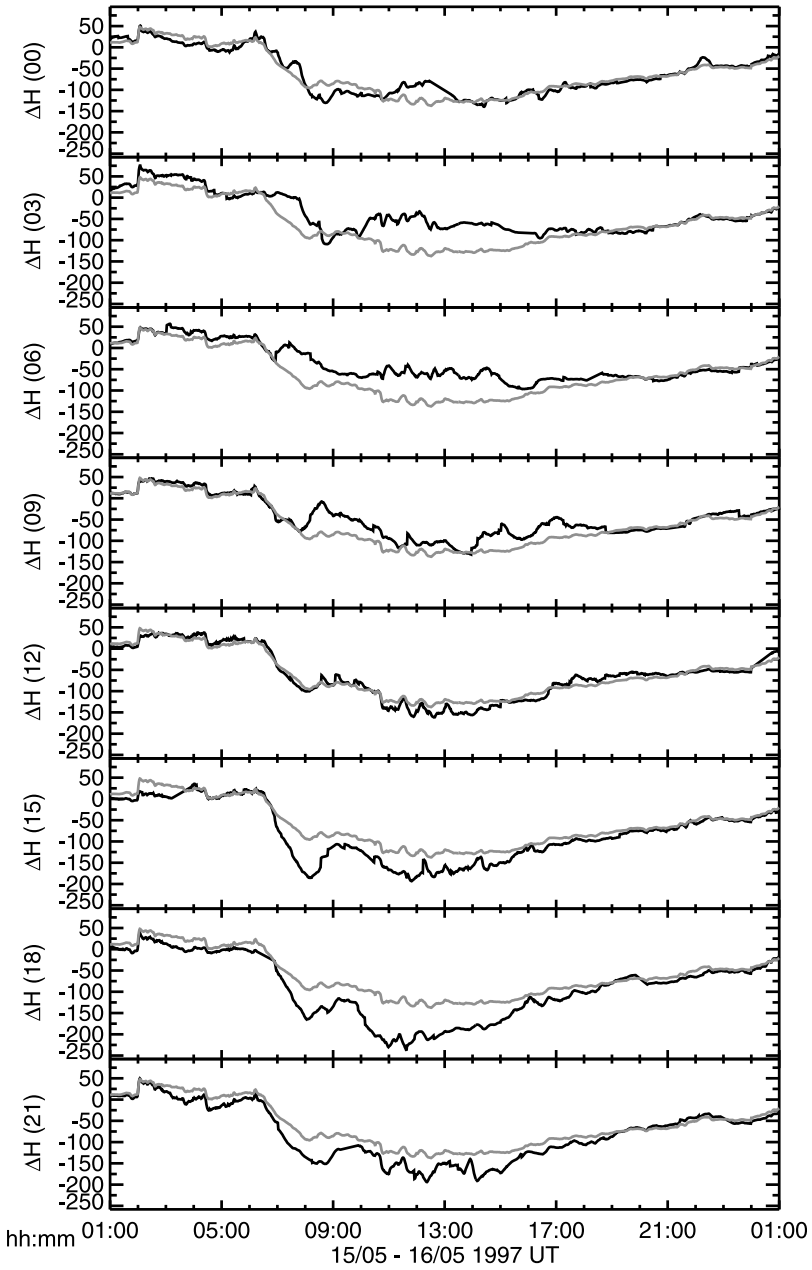


**Figure 2.** H variations for the magnetic storm on 15 May 1997 at eight sectors of different magnetic local times. The gray line represents the mean H variations, $\Delta H_m$. The number in the bracket is the magnetic local time.

[16] We analyzed 299 magnetic storms from 1996 to 2006, obtaining the MLT-dependent H variations statistically. Then we further estimate the contribution of the partial ring current to the SYMH index.

## 3. Observations of the Dawn-Dusk Asymmetry

### 3.1. Two Examples

[17] During the ring current injection of a magnetic storm, ions are mostly present in the dusk and premidnight sectors of the Earth because of duskward drifting and therefore produce a highly asymmetric geomagnetic disturbance with magnetic local times. It is expected that the ring current is asymmetric during the main phase and turns to symmetric in the recovery phase.

[18] Figure 2 shows the profiles of H variations with different MLTs for the intense magnetic storm on 15 May 1997, with the minimum SYMH = −129 nT. From top to bottom are shown the H variations at eight sectors with 3-hour uniformly spaced differences in sequence. The eight 3-h bins are 1.5–4.5, 4.5–7.5, 7.5–10.5, 10.5–13.5, 13.5–16.5, 16.5–19.5, 19.5–22.5, 22.5–1.5 in MLT. The number in the bracket is the mean value of MLT. For a given sector, the local H variation is obtained from averaging all

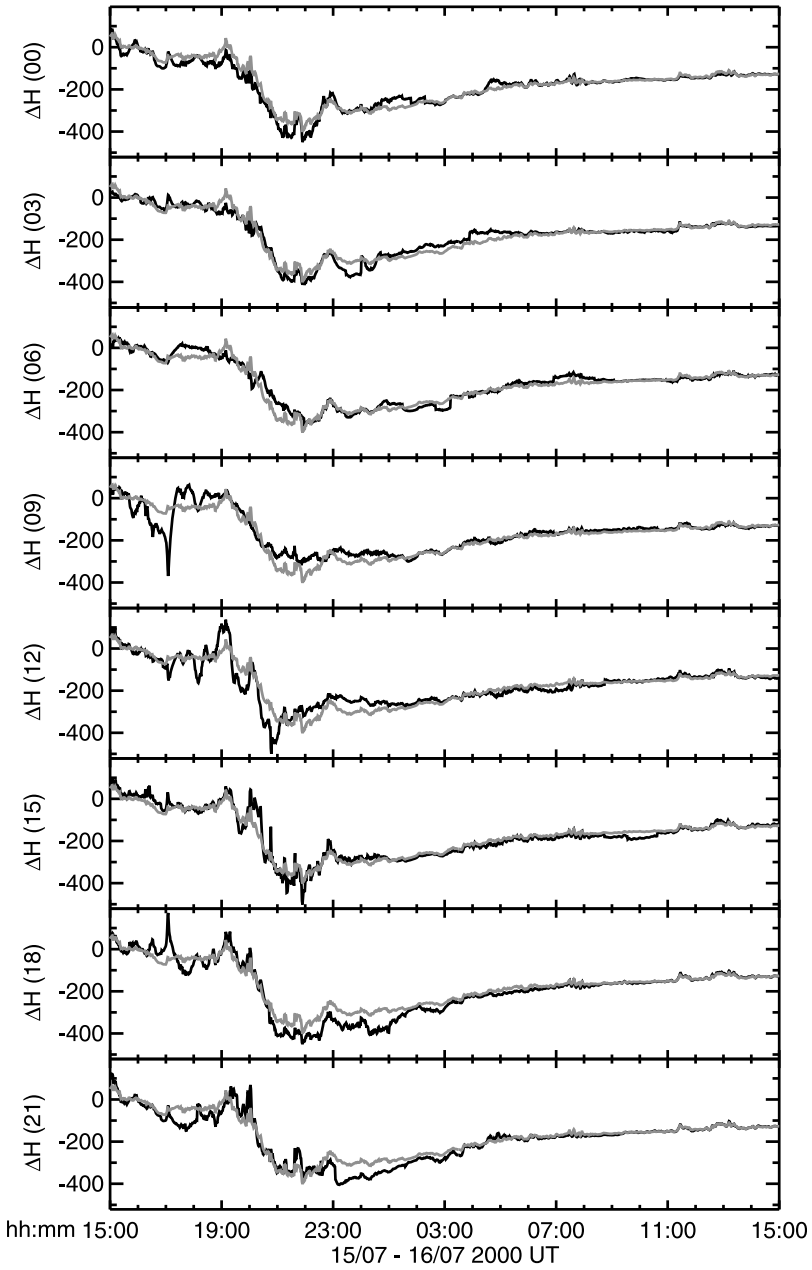


**Figure 3.** H variations for the magnetic storm on 15 July 2000 at eight sectors of different magnetic local times. The gray line represents the mean H variations, $\Delta H_m$. The number in the bracket is the magnetic local time.

the $\Delta H$ observed by the stations which locate in that sector, which is denoted by the black solid line. The gray line denotes the corresponding mean H variations ($\Delta H_m$) for all the 25 stations at each moment. Before $\Delta H_m$ starts to decrease at about 06:00 UT, the H variations at all sections are more or less the same during the quiet period and the initial phase. Since the beginning of the main phase, $\Delta H$s at the dawn sectors are much larger than $\Delta H_m$, while $\Delta H$s at the dusk sectors are much smaller than $\Delta H_m$, which presents a clear dawn-dusk asymmetry. The dawn-dusk asymmetry keeps developing to its maximum until the *SYMH* reaches its minimum and then starts to weaken gradually. At last, the dawn-dusk asymmetry even disappears in the later recovery phase after 19:00 UT. The subsequent differences of H variations between the dawn and dusk sectors become negligible.

[19] To study the asymmetry quantitatively, we define a parameter ($\xi$) to describe the degree of the dawn-dusk asymmetry, given by

$$\xi = \left| \frac{\Delta H_{\max} - \Delta H_{\min}}{\Delta H_m} \right| \tag{3}$$

where $\Delta H_{\max}$ is the maximum H depression at the dawn sector (03:00–07:00 MLT), and $\Delta H_{\min}$ is the minimum H depression at the dusk sector (17:00–21:00 MLT). When $\xi = 0$, it suggests that there is no dawn-dusk asymmetry. The larger $\xi$ is, the stronger dawn-dusk asymmetry occurs. For the

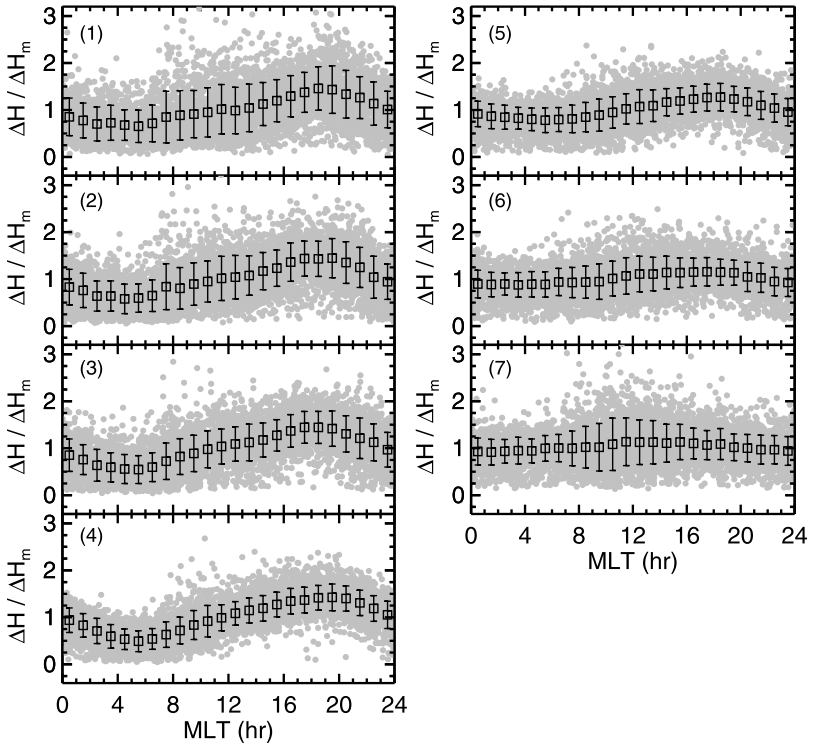


**Figure 4.** Correlations between the relative H variations and magnetic local times at different storm stages for all the magnetic storms. The gray dots represent the observations, and the squares are the averaged values for every magnetic local time. The short vertical lines represent the errors and the standard deviations of the data are averaged.

storm on 15 May 1997, the asymmetric degree is ~1.36 when SYMH reaches its minimum.

[20] Figure 3 shows another example, the superstorm on 15 July 2000 with the minimum SYMH = −347 nT. The plots are as the same as Figure 2. The evolving characteristics of the dawn-dusk asymmetry are similar to the previous one. However, the dawn-dusk asymmetric degree is much weaker. The asymmetric degree is only ~0.29 when SYMH reaches its minimum. Further analysis shows that the degree of the dawn-dusk asymmetry is correlated with the storm intensity, which will be shown in section 3.3.

### 3.2. Development of the Dawn-Dusk Asymmetry During Magnetic Storms

[21] To study the evolution of the above mentioned dawn-dusk asymmetry in detail, we divide the temporal development of a magnetic storm into seven stages and then perform a statistical analysis. The seven stages are the time intervals when (1) the SYMH index first decreases to one third of its minimum during the main phase; (2) the SYMH index first decreases to one half of its minimum during the main phase; (3) the SYMH index first decreases to two thirds of its minimum during the main phase; (4) the SYMH index decreases to its minimum; (5) the SYMH index first increases to two thirds of its minimum during the recovery phase; (6) the SYMH index first increases to one half of its minimum during the recovery phase; (7) the SYMH index first increases to one third of its minimum during the recovery phase. Thus stages 1–3 describe the development of the main phase, stage 4 represents the storm peak, and stages 5–7 describe the development of the recovery phase.

[22] For a magnetic storm, we can obtain the observations of relative H variations ($\Delta H/\Delta H_m$) at 25 stations for all the storm stages. If there are no measurements for any stations, no treatments will be operated. Figure 4 shows the statistical results of the relative H variations at different storm stages for all the 299 magnetic storms. The relative H variations are shown by the grey dots. To reflect the whole developing characteristics of relative H variations with MLTs, we averaged the grey dots for every MLT, and the results are shown in the squares. Every station is weighted equally in the averaging. The short vertical lines represent the errors, which are the standard deviations of averaging.

[23] At the beginning of the main phase of magnetic storms, stage 1 in Figure 4, a significant dawn-dusk asymmetry has already formed. At the dawn sector, the relative H variations are less than 1, with the minimum in 05:00–06:00 MLT bin. While at the dusk sector, the relative H variations are larger than 1, peaking in 18:00–19:00 MLT bin. The relative difference between the maximum and the minimum of $\Delta H$ reflects the degree of the dawn-dusk asymmetry. The greater relative difference is, the more significant dawn-dusk asymmetry is. As time goes on, the dawn-dusk asymmetry also develops accordingly. At first, the dawn-dusk asymmetry gradually strengthens until the SYMH index reaches its minimum. Then, it quickly weakens in the recovery phase. In the later recovery phase, the relative H variations approximately equal 1 for both the dawn and dusk sectors, implying the disappearance of the dawn-dusk asymmetry. At that time, the relative H variations

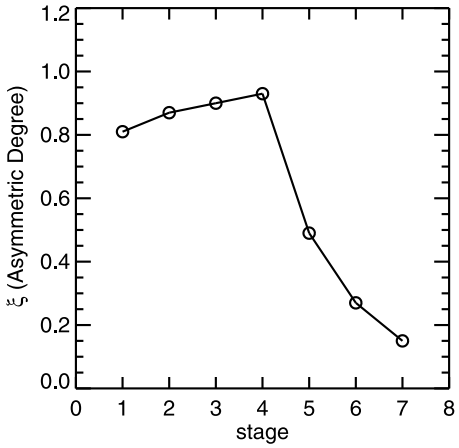


**Figure 5.** Evolution of the degree of dawn-dusk asymmetry for all the storms during different stages of storm intensification as defined in section 3.2. Stages 1–3 describe the development of the main phase, stage 4 represents the storm peak, and stages 5–7 describe the development of the recovery phase.

near the magnetic local noon are relatively a little larger, which is probably due to the decrease of the northward induced magnetic field by the magnetopause currents as a result of both the decrease of the magnetopause current magnitude and the sunward shifting of the dayside magnetopause. It should be pointed out that the relative H variations at the beginning of the main phase exhibit a bit scatter from the baseline (the line connecting the squares), which may infer that there does not exist a clear dawn-dusk asymmetry for some storms. As the development of magnetic storms, the relative H variations become more concentrated to the baseline, and the errors also decrease accordingly, which may infer that there exists a clear significant dawn-dusk asymmetry for most of the storms. This further indicates the evolution of the dawn-dusk asymmetry. Similar to Figure 4, Figure 5 shows the correlation between the degree of the dawn-dusk asymmetry ($\xi$) and the storm stages as defined above, demonstrating the corresponding evolution of $\xi$ during the development of magnetic storms more clearly.

### 3.3. Storm Intensity Effect

[24] From the comparison of two examples shown in section 3.1, it seems that the dawn-dusk asymmetry is weaker for the superstorm than the intense storm. In this section, we will study the effect of storm intensity on the dawn-dusk asymmetry. We divide the 299 magnetic storms into three groups, moderate storms with $-100 < \text{SYMH} \leq -50$ nT, intense storms with $-300 < \text{SYMH} \leq -100$ nT, and super storms with $\text{SYMH} \leq -300$ nT. In our previous work, *Li et al.* [2010] found that the dayside magnetopause moves earthward of the synchronous orbit for storms with $\text{SYMH} \leq -300$ nT by using the 360° panoramic synthesis technique. Therefore we still define the magnetic storms with $\text{SYMH} \leq -300$ to be super storms in this study.

[25] From left to right, Figure 6 shows the correlations between relative H variations and MLTs at different storm stages for all the three groups successively. For moderate and intense storms, the evolving characteristics of the dawn-dusk asymmetry are more or less as the same as above-summarized ones for all the magnetic storms. For super storms the evolving characteristics are similar too, although the dawn-dusk asymmetry is weaker. Take stage 4, for example, the degree of dawn-dusk asymmetry becomes weaker and weaker as the storm intensity increases.

[26] Figure 7 shows the evolutions of $\xi$ for three groups of magnetic storms with different intensity. The triangles, squares, and circles represent the moderate, intense, and super storms, respectively. It is noted that the relative H variations have been smoothed with a width of three points to abate the adverse effect of oscillations in calculating the asymmetric degrees for super storms. Except a slight decrease of the asymmetric degree at stage 4 for intense storms, the evolving characteristics of $\xi$ for all the three groups are more or less the same as that for all the storms summarized before. The asymmetric degree first increases gradually until the *SYMH* index reaches its minimum and then rapidly decreases in the recovery phase. At the later recovery phase, the dawn-dusk asymmetry is quite weak. In particular, the asymmetric degree exhibits a storm intensity dependence relationship. The corresponding asymmetric degree decreases with the increasing of storm intensity.

## 4. Estimating Partial Ring Current Contribution

[27] In general, the symmetric ring current causes almost identical magnitudes of H depressions for all the MLTs, and the cross-tail current locates in the night sector, causing a weak day-night asymmetric H depressions. In conclusion, the partial ring current is responsible for the dawn-dusk asymmetry shown in section 3.

[28] The energy density distribution of the partial ring current peaks near dusk, from both observations [*Lui*, 2003; *Le et al.*, 2004; *Jorgensen et al.*, 2004; *Anderson et al.*, 2005; *Shi et al.*, 2006] and simulations [*Liemohn et al.*, 2001b; *Ebihara et al.*, 2002; *Jordanova et al.*, 2003], leading to a strong dawn-dusk asymmetric H depression. From Figure 4 and Figure 6, it is also clear that the statistical relative H variation peaks in 18:00~20:00 MLT with its minimum in 04:00~06:00 MLT. This implies that the partial ring current locates in the dusk-to-midnight sector, peaking in 18:00~20:00 MLT.

[29] In the next estimation, we adopted the model of the partial ring current as follows: (1) the partial ring current locates in the dusk sector, with an angle between its center and midnight of $\beta$; (2) the partial ring current has a longitudinal extension of $\alpha$ in MLT; (3) the current density of partial ring current ($I_{PRC}$) is equal at different MLT; (4) the equivalent radial distance of partial ring current ($L_P$) is dependent on the storm intensity.

[30] Considering the H depressions at 18:00 MLT and 06:00 MLT, where the integrated effects of the symmetric ring current and cross-tail current are equal to each other, we can obtain that

$$\gamma_1 = \frac{(1+\kappa)(B_{P1} + B_{SR} + B_{CT})}{\Delta H_m} \tag{4}$$

$$\gamma_2 = \frac{(1+\kappa)(B_{P2} + B_{SR} + B_{CT})}{\Delta H_m} \tag{5}$$

where $B_{P1}$ and $B_{P2}$ are the magnitudes of H depression caused by the partial ring current at 18:00 MLT and

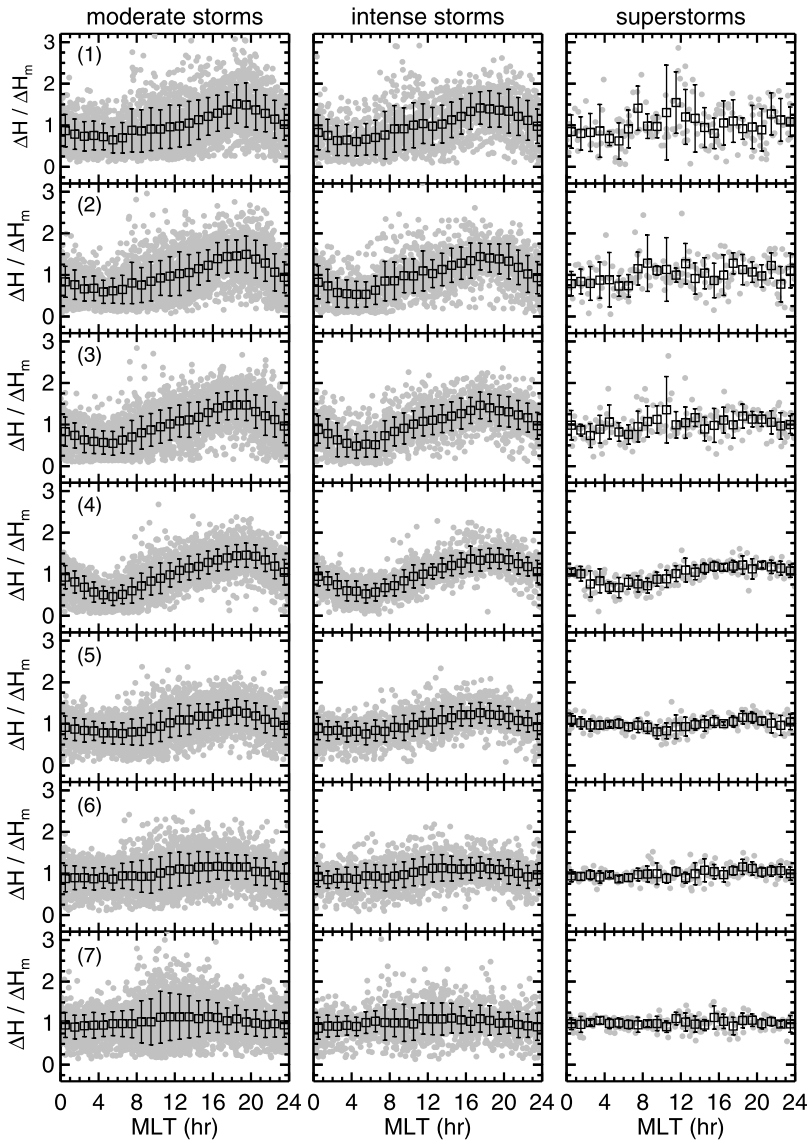


**Figure 6.** Correlations between the relative H variations and magnetic local times at different storm stages for the magnetic storms with different intensities.

06:00 MLT, respectively; $B_{SR}$ and $B_{CT}$ are the magnitudes of H depression caused by the symmetric ring current and cross-tail current, respectively; $\gamma_1$ and $\gamma_2$ are the relative H variations at 18:00 MLT and 06:00 MLT, respectively; $\kappa$ represents the effect of currents induced inside the Earth and is considered to be ~0.3 [*Langel and Estes*, 1985; *Häkkinen et al.*, 2002].

[31] $B_{P1}$ and $B_{P2}$ can also be obtained from Biot-Savart Law based on the above model of the partial ring current, given by

$$B_{P1} = \frac{\mu_0 I_{PRC}}{4\pi} \int_{-\alpha/2}^{\alpha/2} \frac{L_p[L_P - r_0 \sin(\theta+\beta)]}{\left[(L_P)^2 + (r_0)^2 - 2r_0 L_P \sin(\theta+\beta)\right]^{3/2}} d\theta \quad (6)$$

$$B_{P2} = \frac{\mu_0 I_{PRC}}{4\pi} \int_{-\alpha/2}^{\alpha/2} \frac{L_p[L_P + r_0 \sin(\theta+\beta)]}{\left[(L_P)^2 + (r_0)^2 + 2r_0 L_P \sin(\theta+\beta)\right]^{3/2}} d\theta \quad (7)$$

where $r_0$ is the Earth's radii. The averaged H depression caused by the partial ring current for all the MLTs, $B_P$, is

$$B_P = \frac{1}{2\pi} \frac{\mu_0 I_{PRC}}{4\pi} \int_0^{2\pi} \int_{-\alpha/2}^{\alpha/2} \cdot \frac{L_p[L_P - r_0 \sin(\theta+\beta)]}{\left[(L_P)^2 + (r_0)^2 - 2r_0 L_P \sin(\theta+\beta)\right]^{3/2}} d\theta d\beta. \quad (8)$$

[32] The contribution of the partial ring current to the mean H variation, $\eta$, is determined by

$$\eta = \frac{B_P}{\Delta H_m} \times 100\% \quad (9)$$

Substituting equations (4) and (5) into equation (9) yields

$$\eta = \frac{B_P(\gamma_1 - \gamma_2)}{(1+\kappa)(B_{P1} - B_{P2})} \times 100\% \quad (10)$$

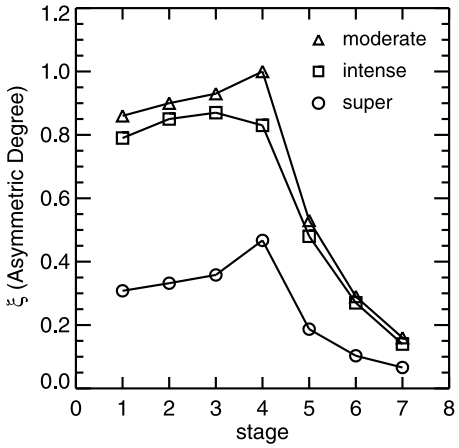


**Figure 7.** Evolution of the degree of dawn-dusk asymmetry for magnetic storms with different intensities. The seven stages of storm intensification have been defined in section 3.2.

If $L_P$, $\alpha$, and $\beta$ are determined, we can calculate $B_{P1}$, $B_{P2}$, and $B_P$ from equation (6), (7), and (8), respectively. Besides, $\gamma_1$ and $\gamma_2$ can be obtained from our previous statistical analysis. Substituting $B_{P1}$, $B_{P2}$, $B_P$, $\gamma_1$, and $\gamma_2$ into equation (10), we can then obtain the partial ring current's contribution, $\eta$.

[33] From Figure 4 and Figure 6, it is clear that the statistical relative H variation peaks in 18:00~20:00 MLT with its minimum in 04:00~06:00 MLT, which is also consistent with the findings of *Le et al.* [2004], *Anderson et al.* [2005], and *Shi et al.* [2006]. We hence assume $\beta$ = 80° in our calculation. Besides, the previous studies showed that the longitudinal widths of partial ring current were ~90°–180° [e.g., *Cummings*, 1966; *Kamide and Fukushima*, 1971; *Crooker and Siscoe*, 1974]. In practice, we assume $\alpha$ to be 120°.

[34] *Mauk and McIlwain* [1974] summarized an empirical formula of the correlation between the inner boundary of the ring current and $K_P$ index as follows:

$$L_b = \frac{122 - 10K_P}{LT - 7.3} \tag{11}$$

where $L_b$ is the inner boundary of ring current and $LT$ is local time. For all the magnetic storms, the mean $K_P$ index is ~6, and the inner boundary of ring current at midnight ($LT$ = 24) is calculated to be 3.74 $R_E$. For the moderate, intense, and super storms, the mean $K_P$ index is about 5+, 7, 9−, and the mean $L_b$ at midnight is 4.11 $R_E$, 3.10 $R_E$, and 2.02 $R_E$, respectively. $L_b$ is the innermost extent of the hot ions, while $L_P$ represents the radial distance of the partial ring current. $L_P$ must be farther away from the Earth's center than $L_b$. However, $L_b$ is obtained from empirical formula. For simplicity, we roughly assume that $L_P \simeq L_b$ in this study.

[35] Figure 8a shows the contribution of the partial ring current to Dst for all the magnetic storms. During the main phase, the partial ring current is the dominant contributor to *Dst*, and the contribution increases gradually as the SYMH index keeps decreasing. When the SYMH index reaches its minimum, the contribution of the partial ring current reaches its maximum too. The peak contribution is ~75%. During the recovery phase, the contribution of the partial ring current starts to decrease rapidly. At the later recovery phase, the partial ring current is no longer the key contributor and its contribution even can be neglected. Figure 8b shows the contribution of the partial ring current to Dst for the moderate, intense, and super storms. On the whole, the evolving characteristics of the partial ring current's contribution for these three groups are similar to that for all the magnetic storms shown in Figure 8a. The partial ring current is still the key contributor to Dst in the main phase of moderate and intense storms. However, it is no longer dominant in the main phase of super storms. The corresponding contribution of the partial ring current decreases when the storm intensity increases. The peak contributions for the moderate, intense, and super storms are ~87%, ~58%, and ~21%, respectively.

[36] Figure 9 shows the percentage of magnetic storms for which the contribution of the partial ring current exceeds 50% when the SYMH index reaches its minimum. It is clear that the percentage of magnetic storms with a dominant contribution from the partial ring current decreases as the storm intensity increases gradually.

## 5. Discussion

[37] Previous studies have not yet reached an agreement on which magnetospheric current system contribute the most to the storm-time Dst variation. This is our original

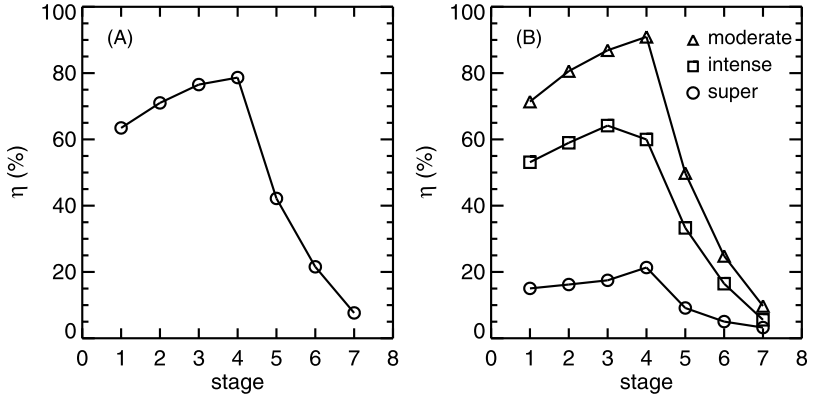


**Figure 8.** Contribution of partial ring current to the SYMH index, (a) for all storms in the database and (b) for the moderate, intense, and super storms.

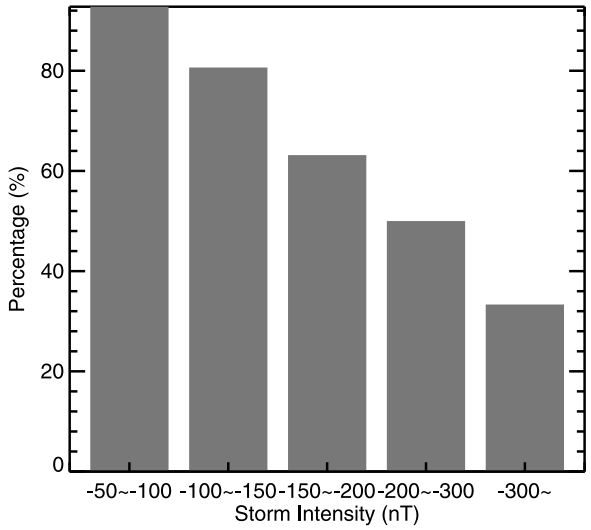


**Figure 9.** Percentage of magnetic storms, for which the contribution of partial ring current exceeds 50% when the SYMH index reaches its minimum.

motivation. The four major current systems, which can contribute to the geomagnetic H depression, have different origin, topology, and effect. This makes it possible to validate which one is the predominant contributor by investigating the distribution of geomagnetic depression with magnetic local times. If there is no significant longitudinal asymmetry of geomagnetic disturbance, it infers that the symmetric current is predominant in the developing of magnetic storms. If there is a strong day-night asymmetry, it infers that the cross-tail current is significant. And if there is a strong dawn-dusk asymmetry, it infers the dominant contribution of partial ring current.

[38] The low-latitude dawn-dusk asymmetric geomagnetic disturbance field has been found to be so prominent during the main and early recovery phase of a magnetic storm and has been traditionally attributed to a dusk-centered partial ring current. Both observations [*Lui*, 2003; *Le et al.*, 2004; *Jorgensen et al.*, 2004; *Anderson et al.*, 2005; *Shi et al.*, 2006] and simulations [*Liemohn et al.*, 2001b; *Ebihara et al.*, 2002; *Jordanova et al.*, 2003] lead to the conclusion that the partial ring current peaks near dusk, leading to a strong dawn-dusk asymmetric H depression. Our results from statistical analysis of 299 magnetic storms are consistent with the above findings. This does not contradict the reports of postmidnight enhancement (PME) [e.g., *Brandt et al.*, 2002; *Fok et al.*, 2003; *Ebihara and Fok*, 2004; *Perez et al.*, 2004; *Buzulukova et al.*, 2010]. The explanation of the difference between location of partial ring current peak and ENA peak is given by *Buzulukova et al.* [2010]. They showed that PME is formed in a particular energy range depending on the strength of the storm. They also concluded that PME is often produced by ions with energies below ~16 keV for moderate storms and ~60 keV for strong storms, while most of the ring current pressure is produced by ions with energies above ~16 keV for moderate storms and ~60 keV for strong storms.

[39] *Liemohn et al.* [2001a, 2001b] analyzed four magnetic storms, concluding the dominant role of partial ring current in producing the storm-time Dst variations. *Le et al.* [2004] derived three-dimensional current density by examining the 20 years of magnetospheric magnetic field data from ISEE, AMPTE/CCE, and Polar missions, finding that the partial ring current was three times of symmetric ring current under moderate magnetic storms. Our estimation of partial ring current contribution obtained from dawn-dusk asymmetry is consistent with their findings. However, our statistical analyses of a large number of magnetic storms are able to give the quantitative evolution of the partial ring current at different storm stages.

[40] *Weygand and McPherron* [2006] utilized 1-min resolution SYMH and ASYH indices to study the dependence of ring current asymmetry on storm phase. They found that the symmetric and partial ring currents grow together during the main phase, and the main phase current system is converted to a symmetric ring as the ring current decays. Our results are consistent with that. Besides, the effect of storm intensity on the partial ring current contribution is also studied here. We found that the contribution of partial ring current weakens gradually as the storm intensity increases. It is no longer predominant for super storms. At that time, the SYMH index is mainly caused by the symmetric ring current. It could be understood physically. The partial ring current is partly closed onto the Region-2 field-aligned current and partly flows from the magnetotail into the inner magnetosphere and then out to the magnetopause. During more intense storms, the ring current injection ions would have higher energy. Thus more injection ions would tend to form a symmetry ring current circuit around the Earth. Moreover, the Region-2 field-aligned current may saturate during super storms. These make the partial ring current saturate. *Lopez et al.* [2009] found that the ring current does not saturate during intense storms. In their study they did not distinguish the symmetric ring current and partial ring current, which infers that the symmetric ring current could increase without the saturation phenomenon. Hence the contribution of the partial ring current is no longer predominant.

[41] To make the estimation of the partial ring current contribution, a relatively realistic model of the partial ring current was adopted. Uncertainties in the estimation result mainly from the assumptions of the partial ring current model. If other parameters are fixed, the partial ring current contribution will increase nearly linearly with $\alpha$ and $L_P$, and decrease gradually with $\beta$, as shown in Figure 10. The more realistic partial ring current in the future would be needed and helpful in estimating the contribution of the partial ring current more accurately.

## 6. Summary

[42] To identify which magnetospheric current system contributes the most to the SYMH index during magnetic storms, we performed a statistical analysis of 299 magnetic storms from 1996 to 2006 and investigated the distribution of the H depressions with magnetic local times (MLT), by using data from 25 geomagnetic stations distributed almost uniformly in magnetic longitudes over magnetic latitudes ranging from 9° to 45°. As expected, there exists a significant dawn-dusk asymmetry of H depression during the storm main phase and early recovery phase for most of the magnetic storms. With further analysis, we obtain the

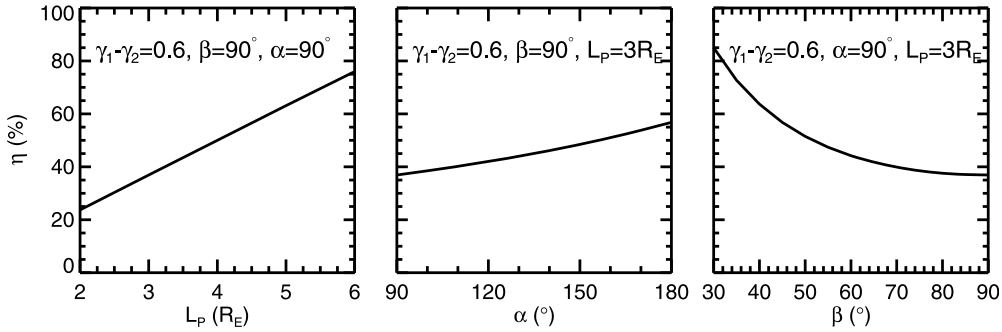


**Figure 10.** Effect of Ł$_P$, $\alpha$, and $\beta$ on estimating the partial ring current contribution with other parameters fixed.

evolving characteristics of the dawn-dusk asymmetry during the development of magnetic storms. It forms at the beginning of the main phase and gradually strengthens until the SYMH index reaches its minimum. In the recovery phase, the dawn-dusk asymmetry starts to weaken rapidly and even disappears in the later recovery phase. What needs to be stressed is that the asymmetric degree decreases as the storm intensity increases, although the evolving characteristics for the magnetic storms with different intensity are similar.

[43] Generally, the symmetric ring current causes almost identical magnitudes of H depressions for all the MLTs, and the cross-tail current locates at the night sector, causing a weak day-night asymmetric H depressions. Far more likely, the partial ring current is responsible for the dawn-dusk asymmetry. The signature of the dawn-dusk asymmetry suggests that the partial ring current locates in the dusk-to-midnight sector, peaking in 18:00~20:00 MLT. On the basis of the observations of the dawn-dusk asymmetry and some reliable assumptions of the partial ring current model, we first obtain the quantitative evolving characteristics of the contribution of partial ring current to Dst during the development of magnetic storms through equation (10). Indifferent stages of a magnetic storm, the magnetospheric current system which contributes the most to Dst is different too. During the main phase, the contribution of the partial ring current is predominant, and the percentage gradually increases until the SYMH index reaches its minimum, while during the recovery phase, the contribution of the partial ring current decreases rapidly and can be neglected in the later recovery phase. Further analysis shows that the corresponding contributions of the partial ring current decreases gradually as the storm intensity increases. For moderate storms, the peak contribution of the partial ring current is ~87%; for intense storms, the peak contribution slightly reduces to ~58%; and for super storms, the peak contribution keeps on dropping to ~21%. Considering the closure of the partial ring current, we suggest that it is because of more injection ions tend to form the symmetric ring current and the saturation of the Region-2 field-aligned current as storm intensity increases.

[44] **Acknowledgments.** The results presented in this paper rely on data collected at magnetic observatories. We thank the national institutes that support them and INTERMAGNET for promoting high standards of magnetic observatory practice (www.intermagnet.org). This work was supported by grants NNSFC 40921063, 40831060, 40974106 and in part by the Specialized Research Fund for State Key Laboratories of China.

[45] Masaki Fujimoto thanks the reviewers for their assistance in evaluating this paper.

## References

Alexeev, I. I., V. V. Kalegaev, and Y. I. Feldstein (1992), Modeling of magnetic field in the strongly disturbed magnetosphere (in Russian), *Geomagn. Aeron.*, *32*(4), 8–14.

Alexeev, I. I., E. S. Belenkaya, V. V. Kalegaev, Y. I. Feldstein, and A. Grafe (1996), Magnetic storms and magnetotail currents, *J. Geophys. Res.*, *101*, 7737–7747.

Alexeev, I. I., V. V. Kalegaev, E. S. Belenkaya, S. Y. Bobrovnikov, Y. I. Feldstein, and L. I. Gromova (2001), Dynamic model of the magnetosphere: Case study for January 9–12, 1977, *J. Geophys. Res.*, *106*, 25,683–25,693.

Anderson, B. J., S. Ohtani, H. Korth, and A. Ukhorskiy (2005), Storm time dawn-dusk asymmetry of the large-scale Birkeland currents, *J. Geophys. Res.*, *110*, A12220, doi:10.1029/2005JA011246.

Belova, E. G., and T. P. Maltsev (1994), Supplementary sources of geomagnetic depression during the geomagnetic storm of 8–9 February, 1986, *J. Atmos. Terr. Phys.*, *56*, 1011–1015.

Brandt, P. C., S. Ohtani, D. G. Mitchell, M.-C. Fok, E. C. Roelof, and R. Demajistre (2002), Global ENA observations of the storm mainphase ring current: Implications for skewed electric fields in the inner magnetosphere, *Geophys. Res. Lett.*, *29*(20), 1954, doi:10.1029/2002GL015160.

Buzulukova, N., M.-C. Fok, J. Goldstein, P. Valek, D. J. McComas, and P. C. Brandt (2010), Ring current dynamics in moderate and strong storms: Comparative analysis of TWINS and IMAGE/HENA data with the Comprehensive Ring Current Model, *J. Geophys. Res.*, *115*, A12234, doi:10.1029/2010JA015292.

Clauer, C. R., and R. L. McPherron (1974), Mapping the local time-universal time development of magnetospheric substorms using mid-latitude magnetic observations, *J. Geophys. Res.*, *79*, 2811–2820.

Clauer, C. R., M. W. Liemohn, J. U. Kozyra, and M. L. Reno (2003), The relationship of storms and substorms determined from mid-latitude ground-based magnetic maps, in *Disturbances in Geospace: The Storm-Substorm Relationship*, *Geophys. Monogr. Ser.*, vol. 142, edited by S. J. Sharma, p. 143–147, AGU, Washington, D. C.

Clauer, C. R., X. Cai, D. Welling, A. DeJong, and M. G. Henderson (2006), Characterizing the 18 April 2002 storm-time saw tooth events using ground magnetic data, *J. Geophys. Res.*, *111*, A04S90, doi:10.1029/2005JA011099.

Crooker, N. U., and G. L. Siscoe (1974), Model geomagnetic disturbance from asymmetric ring current particles, *J. Geophys. Res.*, *79*, 589–594.

Crooker, N. U., and G. L. Siscoe (1981), Birkeland currents as the cause of the low-latitude asymmetric disturbance field, *J. Geophys. Res.*, *86*, 11,201–11,210.

Cummings, W. D. (1966), Asymmetric ring currents and the low-latitude disturbance daily variation, *J. Geophys. Res.*, *71*, 4495–4503.

DeForest, S., and C. E. McIlwain (1971), Plasma clouds in the magnetosphere, *J. Geophys. Res.*, *76*, 3587–3611.

De Michelis, P., I. A. Daglis, and G. Consolini (1999), An average image of proton plasma pressure and of current systems in the equatorial plane derived from AMTE/CCE-CHEM measurements, *J. Geophys. Res.*, *104*, 28,615–28,624.

Dremukhina, L. A., and Y. I. Feldstein (1999), Dst variation of magnetic field during magnetic storms (in Russian), *Geomagn. Aeron.*, *39*(3), 41–46.

Ebihara, Y., and M.-C. Fok (2004), Postmidnight storm-time enhancement of tens-of-keV proton flux, *J. Geophys. Res.*, *109*, A12209, doi:10.1029/2004JA010523.

Ebihara, Y., M. Ejiri, H. Nilsson, I. Sandahl, A. Milillo, M. Grande, J. F. Fennell, and J. L. Roeder (2002), Statistical distribution of the storm-time proton ring current: POLAR measurements, *Geophys. Res. Lett.*, *29*(20), 1969, doi:10.1029/2002GL015430.

Fok, M.-C., et al. (2003), Global ENA image simulations, *Space Sci. Rev.*, *109*, 77–103.

Friedrich, E., G. Rostoker, and M. G. Connors (1999), Influence of the substorm current wedge on the Dst index, *J. Geophys. Res.*, *104*, 4567–4575.

Fukushima, N., and Y. Kamide (1973), Partial ring current models for worldwide geomagnetic disturbances, *Rev. Geophys.*, *11*, 795–853.

Greenspan, M. E., and D. C. Hamilton (2000), A test of the Dessler-Parker-Sckopke relation during magnetic storms, *J. Geophys. Res.*, *105*, 5419–5430.

Häkkinen, L. V. T., T. I. Pulkkinen, H. Nevanlinna, R. J. Pirjola, and E. I. Tanskanen (2002), Effects of induced currents on Dst and on magnetic variations at midlatitude stations, *J. Geophys. Res.*, *107*(A1), 1014, doi:10.1029/2001JA900130.

Iyemori, T., T. Araki, T. Kamei, and M. Takeda (1992), Mid-latitude geomagnetic indices ASY and SYM (provisional), Data Anal. Cent. for Geomagn. and Space Magn., Faculty of Sci., Kyoto Univ., Kyoto, Japan.

Jordanova, V. K., A. Boonsiriseth, R. M. Thorne, and Y. Dotan (2003), Ring current asymmetry from global simulations using a high-resolution electric field model, *J. Geophys. Res.*, *108*(A12), 1443, doi:10.1029/2003JA009993.

Jorgensen, A. M., H. E. Spence, W. J. Hughes, and H. J. Singer (2004), A statistical study of the global structure of the ring current, *J. Geophys. Res.*, *109*, A12204, doi:10.1029/2003JA010090.

Kamide, Y., and N. Fukushima (1971), Analysis of magnetic storms with DR-indices for equatorial ring current field, *Radio Sci.*, *6*, 277–278.

Langel, R. A., and R. H. Estes (1985), Large-scale, near-field magnetic fields from external sources and the corresponding induced internal field, *J. Geophys. Res.*, *90*, 2487–2494.

Le, G., C. T. Russell, and K. Takahashi (2004), Morphology of the ring current derived from magnetic field observations, *Ann. Geophys.*, *22*, 1267–1295.

Li, H., C. Wang, and J. R. Kan (2010), Midday magnetopause shifts earthward of geosynchronous orbit during geomagnetic superstorms with Dst $\leq -300$ nT, *J. Geophys. Res.*, *115*, A08230, doi:10.1029/2009JA014612.

Liemohn, M. W., J. U. Kozyra, M. F. Thomsen, J. L. Roeder, G. Lu, J. E. Borovsky, and T. E. Cayton (2001a), Dominant role of the asymmetric ring current in producing the stormtime Dst, *J. Geophys. Res.*, *106*, 10,883–10,904.

Liemohn, M. W., J. U. Kozyra, C. R. Clauer, and A. J. Ridley (2001b), Computational analysis of the near-Earth magnetospheric current system, *J. Geophys. Res.*, *106*, 29,531–29,542.

Lopez, R. E., J. G. Lyon, E. Mitchell, R. Bruntz, V. G. Merkin, S. Brogl, F. Toffoletto, and M. Wiltberger (2009), Why doesn't the ring current injection rate saturate?, *J. Geophys. Res.*, *114*, A02204, doi:10.1029/2008JA013141.

Love, J. J., and J. L. Gannon (2009), Revised Dst and the epicycles of magnetic disturbance: 1958–2007, *Ann. Geophys.*, *27*, 3101–3131.

Love, J. J., and J. L. Gannon (2010), Movie-maps of low-latitude magnetic storm disturbance, *Space Weather*, *8*, S06001, doi:10.1029/2009SW000518.

Lui, A. T. Y. (2003), Inner magnetospheric plasma pressure distribution and its local time asymmetry, *Geophys. Res. Lett.*, *30*(16), 1846, doi:10.1029/2003GL017596.

Maltsev, Y. P. (2004), Points of controversy in the study of magnetic storms, *Space Sci. Rev.*, *110*, 227–267.

Maltsev, Y. P., and A. A. Ostapenko (2002a), Statistical assessment of the magnetotail current contribution to Dst, paper presented at Sixth International Conference on Substorms, Univ. of Wash., Seattle.

Maltsev, Y. P., and A. A. Ostapenko (2002b), Comments on "Evaluation of the Tail Current Contribution to Dst" by N. E. Turner et al., *J. Geophys. Res.*, *107*(A1), 1010, doi:10.1029/2001JA900098.

Mauk, B., and C. McIlwain (1974), Correlation of Kp with the substorm-injected plasma boundary, *J. Geophys. Res.*, *79*(22), 3193–3196.

Munsami, V. (2000), Determination of the effects of substorms on the storm-time ring current using neural networks, *J. Geophys. Res.*, *105*, 27,833–27,840.

Perez, J. D., X. Zhang, P. C:son Brandt, D. G. Mitchell, J. Jahn, and C. J. Pollock (2004), Dynamics of ring current ions as obtained from IMAGE HENA and MENA ENA images, *J. Geophys. Res.*, *109*, A05208, doi:10.1029/2003JA010164.

Shi, Y., E. Zesta, L. R. Lyons, K. Yumoto, and K. Kitamura (2006), Statistical study of effect of solar wind dynamic pressure enhancements on dawn-to-dusk ring current asymmetry, *J. Geophys. Res.*, *111*, A10216, doi:10.1029/2005JA011532.

Sugiura, M., and T. Kamei (1991), Equatorial Dst index 1957–1986, Int. Serv. for Geomagn. Indices, Saint-Maur-des-Fosses, France.

Turner, N. E., D. N. Baker, T. I. Pulkkinen, and R. L. McPherron (2000), Evaluation of the tail current contribution to Dst, *J. Geophys. Res.*, *105*, 5431–5439.

Turner, N. E., D. N. Baker, T. I. Pulkkinen, J. L. Roeder, J. F. Fennell, and V. K. Jordanova (2001), Energy content in the storm time ring current, *J. Geophys. Res.*, *106*, 19,149–19,156.

Weygand, J. M., and R. L. McPherron (2006), Dependence of ring current asymmetry on storm phase, *J. Geophys. Res.*, *111*, A11221, doi:10.1029/2006JA011808.

J. R. Kan, Geophysical Institute, University of Alaska Fairbanks, Fairbanks, AK 99775, USA. (joe.kan@gi.alaska.edu)

H. Li and C. Wang, State Key Laboratory of Space Weather, Center for Space Science and Applied Research, Chinese Academy of Sciences, PO Box 8701, Beijing 100190, China. (hli@spaceweather.ac.cn; cw@spaceweather.ac.cn)